



Improving crystallization and eruption age estimation using U–Th and U–Pb dating of young volcanic zircon

Zoe Moser¹, Marcel Guillong¹, Chetan Nathwani¹, Kurumi Iwahashi^{1,2}, Razvan-Gabriel Popa¹, and Olivier Bachmann¹

¹Institute of Geochemistry and Petrology, ETH, Zürich, Switzerland

²Geological Survey of Japan, AIST, Tsukuba, Japan

Correspondence: Zoe Moser (moserz@eaps.ethz.ch)

Abstract. Quantifying timescales and establishing robust eruption chronologies is critical for understanding the evolution and hazards of volcanic systems. U–Th disequilibrium dating on zircon is especially valuable for young and active systems (<300 ka). However, there is no consensus on how to calculate U–Th crystallization ages. To address this, we developed a new LA-ICP-MS U–Th–Pb double-dating technique that simultaneously retrieves U–Th and U–Pb ages from the same zircon ablation volume. This method increases confidence in crystallization ages across 150–300 ka, where the resolution of either method alone is limited. We applied this method to the Kos Plateau Tuff, which spans this critical interval, and compared U–Th model age approaches against the well-established U–Pb age calculations. Model ages calculated using the two endmember approaches, either a constant melt composition or a constant zircon–melt U/Th fractionation factor ($f_{U/Th}$), yield similar age spectra when well-estimated values are used. In this context, it is essential to evaluate whether the measured groundmass glass or whole-rock composition truly reflects the zircon-forming melt. This can be assessed by comparison with the youngest isochron intercept on the secular equilibrium line, which provides an independent melt composition estimate. We also evaluated eruption age estimation methods using synthetic U–Th datasets, with increasing uncertainty toward older ages. Bayesian models, particularly those with uniform priors, consistently outperformed weighted mean approaches in terms of accuracy and precision and are therefore recommended for eruption age estimates in volcanic U–Th zircon datasets.

1 Introduction

Quantifying eruption frequencies and timescales associated with magmatic processes is a fundamental goal in volcanology, particularly for long-lived systems leading to caldera-forming eruptions. Reconstructing the eruptive history of such complex systems, with countless eruptions over tens of millennia, presents significant challenges. Establishing a relative stratigraphy can be difficult, as individual volcanic units may not physically overlap. Additionally, large volcanic systems often exhibit very active geothermal systems at the surface, leading to widespread alteration zones (e.g., Yellowstone: Fournier, 1989; Torfajökull: Björke, 2010; Campi Flegrei: Piochi et al., 2021). Such alteration frequently degrades magmatic minerals that would otherwise record magmatic conditions, rendering them ineffective for reconstructing volcanic histories. Zircon, however, is exceptionally resistant to alteration (Watson and Harrison, 1983). And as it incorporates uranium and almost no lead during magmatic

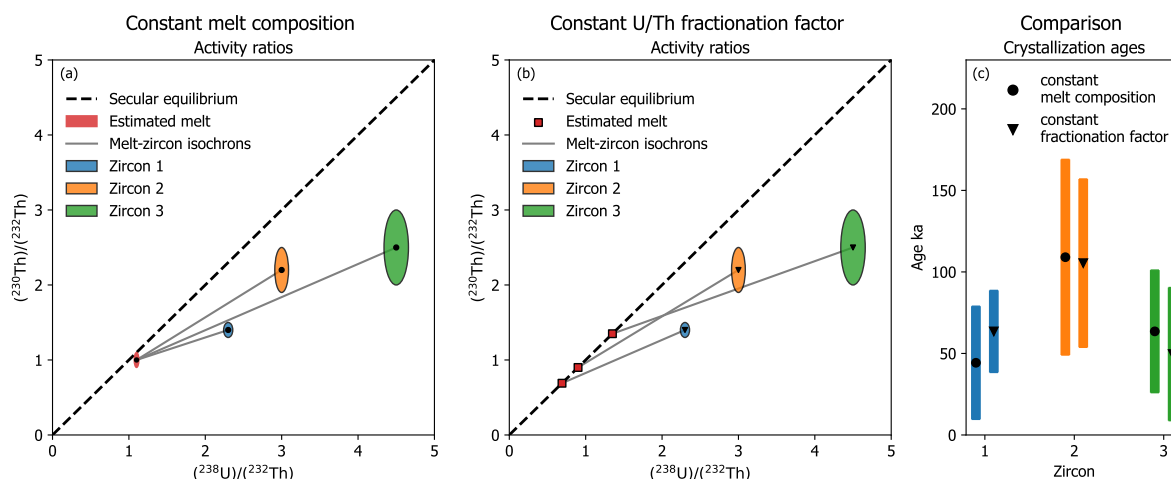


Figure 1. Illustration of two approaches for calculating model U–Th disequilibrium crystallization ages using three synthetic zircon crystals with distinct isotopic signatures. (a) In the first approach, a constant glass composition is assumed to construct individual zircon–melt two-point isochron slopes (Schmitt, 2011). (b) In the second approach, a fixed Th/U fractionation factor between zircon and melt (here 0.20 ± 0.02) is applied to derive the model slope (Boehnke et al., 2016). (c) Resulting crystallization ages from both methods are compared for identical zircon isotopic signatures.

crystallization, it is a useful mineral for dating using the uranium decay systems (Watson and Harrison, 1983). Due to the slow diffusion of elements such as Pb, Th, and U within its crystalline structure, even at magmatic temperatures (Lee et al., 1997), zircon crystals record their crystallization age (Costa, 2008; Bachmann, 2010), providing valuable insights into the duration of magmatic processes, as zircon crystallization can span prolonged periods. Since an accurate chronology is essential for understanding volcanic system evolution, zircon geochronology provides a critical foundation for investigating these dynamic systems.

The most widely used geochronological tools for zircon include U–Pb dating (>150 ka) and U–Th disequilibrium dating (<300 ka). U–Th dating has gained prominence in recent decades (Reid et al., 1997; Coombs and Vazquez, 2014; Locher et al., 2025), yet a debated aspect of U–Th dating of zircon is how to best determine crystallization ages. To calculate these ages, each zircon signal needs to be linked to the melt from which it crystallized to form two-point zircon–melt isochrons. As each zircon model age depends on the melt composition, it is important to estimate this value carefully. Two contrasting ideas dominate as to how the U–Th zircon–melt pair can be approximated (Fig. 1): one idea assumes that a constant isotopic melt composition can be linked to the individual zircon signals (Schmitt, 2011), while the other idea presumes constant U–Th fractionation between zircon and melt, where the melt signature is estimated from the zircon signal itself through a constant U/Th fractionation factor (Boehnke et al., 2016). Choosing between these approaches can have implications for interpreting crystallization histories of volcanic samples.



40 As zircon crystals from single volcanic eruptions typically exhibit dispersed U-Th or U-Pb dates (over kyrs), protracted crystallisation in the underlying magmatic system is dated and not the eruption itself. To directly date the eruption, alternative chronometers such as zircon (U-Th)/He thermochronology can be employed, as they record the time of cooling below the closure temperature of He of $\sim 200^{\circ}\text{C}$ (Reiners et al., 2002), which often corresponds closely to the eruption (e.g., Friedrichs et al., 2020). This dating method comes however with many challenges, including the need for corrections related to initial

45 U-Th disequilibrium, alpha-ejection effects, pre-eruptive residence time, and accounting for internal age and compositional heterogeneity (Friedrichs et al., 2020). Instead of dating the eruption directly, we can infer the eruption age through the latest zircon crystallization, if we assume that zircon crystallized until the eruption took place (Keller et al., 2018; Nathwani et al., 2025). Typical extended zircon crystallization, often reflected in a broad spread of non-overlapping dates within a single sample (Bachmann et al., 2007b), renders global weighted mean and global isochron ages for eruption age estimation unreliable.

50 In contrast, the youngest zircon age generally lacks statistical robustness (Keller et al., 2018). Consequently, alternative approaches have been applied, including weighted mean ages of zircon subsets (e.g., Schoene et al., 2015; Locher et al., 2025) and likelihood-based Bayesian methods (e.g., Cisneros de León et al., 2025; Baudry et al., 2024). Keller et al. (2018) pioneered the application of Bayesian statistics for eruption age estimation from a distribution of zircon U-Pb dates. They found that this method produces superior accuracy and estimates of uncertainty relative to weighted mean or youngest zircon approaches.

55 However, their study focused on ID-TIMS U-Pb data with low variability in uncertainties, a scenario applicable to U-Pb but not to U-Th datasets. In U-Th disequilibrium dating, uncertainties increase for older ages due to the exponential convergence toward secular equilibrium (Schmitt, 2011). Despite the growing number of studies using U-Th zircon data, a range of eruption age estimation methods are currently employed without a systematic evaluation of which approach yields the most reliable results.

60 To improve the application of U-Th zircon dates for quantifying eruption frequencies and timescales, we first evaluate the two opposing model age approaches, followed by an assessment of different eruption age estimation methods tailored to typical LA-ICP-MS U-Th zircon datasets. We test the consistency between methods to calculate zircon crystallization ages, using a combined LA-ICP-MS method that measures U, Th, and Pb isotopes in zircons from the Kos Plateau Tuff (KPT), which exhibit crystallization ages ranging from ~ 160 to >300 ka (Guillong et al., 2014; Bachmann et al., 2007a). By comparing co-recorded

65 U-Pb and U-Th ages from the same ablation volume, we assess the reliability of different U-Th age determination techniques. To further evaluate eruption age estimation methods, we apply them to synthetic U-Th age datasets that simulate typical LA-ICP-MS uncertainties (Fig. 2). In addition, we analyze three samples with independently well-constrained eruption ages, which serve as benchmarks to validate both the model age and eruption age approaches.

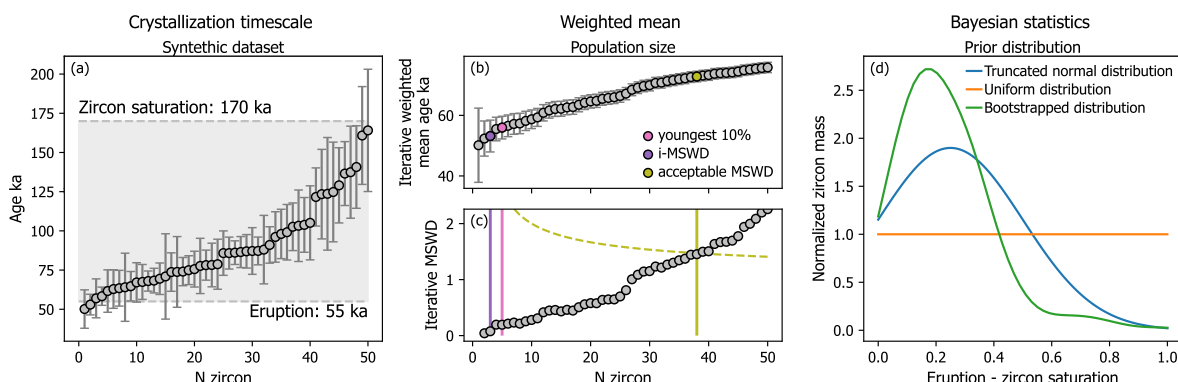


Figure 2. Example of a synthetic U–Th LA–ICP–MS zircon crystallization age dataset and comparison of eruption age estimation methods. (a) Synthetic ranked dataset of 50 zircon crystallization ages, simulating a natural volcanic system with ages skewed toward the eruption. Ages range from a true eruption age of 55 ka to a zircon saturation age of 170 ka and include typical LA–ICP–MS uncertainties. (b) Iteratively calculated weighted mean ages. (c) Corresponding iterative MSWD values, shown alongside tested zircon age subsets used to estimate the eruption age using the weighted mean approach. (d) Zircon age distributions between zircon saturation and eruption tested as prior distributions for the likelihood-based Bayesian eruption age model.

2 Methods

2.1 U–Th(–Pb) dating

2.1.1 Samples

To assess the different methods of calculating the U–Th crystallization ages, we developed a new dating routine to simultaneously measure U–Th–Pb, and to compare the differently calculated U–Th ages with the U–Pb ages of the same ablation volume. To do this, we analysed zircon from the Kos Plateau Tuff, with prolonged zircon crystallization between roughly 160–300 ka (Guillong et al., 2014; Bachmann et al., 2007a). This age range is at the upper limit of potential U–Th age determination (Schmitt, 2011) and on the lower limit of U–Pb age resolution (Guillong et al., 2014). Given that the U–Pb dating is better understood and the underlying uncertainties are better constrained (Sakata et al., 2017; Pollard et al., 2023), the U–Pb age can be used as a benchmark to evaluate how different U–Th model age methods perform. Using additional U–Th measurements and published U–Th data, we then validate these approaches by applying the best model age calculation methods for samples with well-constrained eruption ages. We chose to analyse one sample from the historic Heisei eruption of Mount Unzen in Japan between 1991–1995 and two samples, Laugahraun and Thórsmörk, from the Torfajökull volcanic system in Iceland. Laugahraun is a young lava, which erupted at 1480 ± 11 CE, determined through soil thickening rates and tephrochronology (Larsen, 1984). Thórsmörk is an ignimbrite which has been independently dated through Ar–Ar measurements of glassy fiamme to an age of 56.14 ± 0.44 ka (2σ) by Groen and Storey (2022) and to an age of 51.3 ± 4.2 ka (2σ) by Moles et al. (2019), as well as to



Table 1. LA-ICP-MS strategy for the three methods applied in this study.

| Method | U-Th-Pb zircon | U-Th zircon | U-Th groundmass glass |
|--------------------------------|---|---|------------------------------------|
| Energy density | $\sim 2 \text{ Jcm}^{-2}$ | $\sim 2 \text{ Jcm}^{-2}$ | $\sim 3.5 \text{ Jcm}^{-2}$ |
| Repetition rate | 5 Hz | 5 Hz | 5 Hz |
| Spot size | 29 μm | 29 μm | 163 μm |
| Ablation duration | 40 s | 40 s | 40 s |
| Background duration | 30 s | 30 s | 30 s |
| Masses measured | Pb206, Pb207, Th230, Th232, U235, U238 | 228 ^a , Th230, Th232, U235, U238 | Th230, Th232, U234, U235, U238 |
| Dwell times | 50 ms, 50 ms, 100 ms, 11 ms, 11 ms, 11 ms | 50 ms, 150 ms, 20 ms, 25 ms, 11 ms | 150 ms, 22 ms, 50 ms, 22 ms, 22 ms |
| Detection mode ^b | c,c,c,a,c,a | c,c,a,c,a | c,a,c,c,a |
| Magnet mass | 206, 207, 230, 230, 230, 230 | 228, 228, 228, 228, 228 | 230, 230, 230, 230, 230 |
| Primary reference materials | NIST612, 91500, Monazite, Zirconblank | NIST612, 91500, Monazite, Zirconblank | NIST612, Monazite |
| Validation reference materials | AUSZ7-1, GJ-1, Plesovice, FCT | AUSZ7-1, GJ-1, Plesovice, FCT | ATHO-5, BCR2G, BHVO2G |
| Data reduction scheme | U-Pb reduction (young zircon) | U-Th reduction | U-Th reduction |

^a Zr_2O_3 : $^{90}\text{Zr}^{90}\text{Zr}^{16}\text{O}^{16}\text{O}^{16}\text{O}$

^b c: counting, a: analog.

85 55.6±2.4 ka (2 σ) through Ar-Ar measurements of anorthoclase crystals (Guillou et al., 2019), and an annual layer-counted age of a related tephra deposit in the Greenlandic ice core to 55.4±2.4 ka (2 σ) (Svensson et al., 2008). Further, we examined published SIMS U-Th zircon data from the Belford dome, samples SL-25 and SL-51, in the Soufrière Volcanic Complex in Saint Lucia (Schmitt et al., 2010), in combination with whole rock data (Turner et al., 1996) that was used to calculate model ages. The eruption age of this dome was determined by (U-Th)/He dating of zircon to 13.6±0.8 ka (2 σ) (Schmitt et al., 2010).

90 2.1.2 LA-ICP-MS measurement

The measurements were conducted at ETH Zurich with LA-ICP-MS, which couples a 193 nm Resonetics Resolution 155 LR excimer laser ablation system to a Thermo Element XR sector field mass spectrometer. The specific parameters used for U-Th-Pb and U-Th measurements on zircon and U-Th measurements on the groundmass glass are summarised in Table 1. In all cases, masses with high expected countrates, such as ^{232}Th and ^{238}U , were measured with an analog detection mode and a common analog to puls-counting equivalent factor (ACF), while the other masses were measured in puls-counting mode. A repetition rate of 5 Hz, an energy density of $\sim 2 \text{ Jcm}^{-2}$ with an ablation diameter of 29 μm for zircon and an energy density of $\sim 2.5 \text{ Jcm}^{-2}$ with an ablation diameter of 163 μm for the groundmass glass was used. Reference materials such as NIST612, zircon 91500 (Wiedenbeck et al., 1995), monazite, and zircon-blank were measured alongside the unknowns. Additional zircons, AUSZ7-1 (Kennedy et al., 2014), GJ-1 (Jackson et al., 2004), Plesovice (Sláma et al., 2008), FCT (Schmitz and Bowring, 2001), with known U-Pb ages and in secular equilibrium, were measured as secondary reference materials. For the groundmass glass measurement, ATHO-5, BCR2G and BHVO2G were measured as secondary reference materials (Matthews et al., 2011).



2.1.3 U-Th data Processing

Independent of the measuring method, the processing of the U-Th data follows the steps described by Guillong et al. (2016) and was done with a custom Data Reduction Scheme (DRS) written for implementation in the Iolite software (provided as a supplementary file, also applicable for different minerals dated by U-Th disequilibrium). The DRS corrects the data for (1) the abundance sensitivity of ^{232}Th on ^{230}Th , (2) the interference of polyatomic zirconium oxide (Zr_2O_3) with mass 228 on mass 230, (3) the relative sensitivity between the measurement of U and Th, and (4) the mass bias. To account for the zirconium oxide interference during the U-Th-Pb measurement without actively measuring mass 228, counts of mass 230 in a zircon blank were considered. With the measured secondary reference materials, the secular equilibrium condition of $(^{230}\text{Th})/(^{238}\text{U})$ = 1 was evaluated. The groundmass glass was processed similarly with the same DRS, but the correction for the interference of polyatomic zirconium oxide was not necessary.

With the processed data, we further calculated the individual zircon model ages with different methods, which can be grouped into two main categories, both based on a two-point zircon-melt isochron approach (Fig. 1). (1) On the one hand, a constant isotopic melt composition can be assumed to have been in equilibrium with the individual zircon crystals (Schmitt, 2011). This melt composition can be approximated by either measuring the isotopic ratios within the groundmass glass or in the whole rock, or by using an isochron intercept as a melt anchor point. With this in mind, we calculated the two-point zircon-melt isochron ages with different melt-anchor-point considerations: the equilibrium melt composition was approximated (a) through the measured $^{238}\text{U}/^{232}\text{Th}$ and $^{230}\text{Th}/^{232}\text{Th}$ isotopic ratios of the groundmass glass including error propagation, (b) through the measured $^{238}\text{U}/^{232}\text{Th}$ ratio of the glass assumed to be in secular equilibrium (Boehnke et al., 2016) and equating the $^{230}\text{Th}/^{232}\text{Th}$ isotopic ratio to it, thus avoiding their high uncertainties, (c) through IsoplotR given the measured $^{238}\text{U}/^{232}\text{Th}$ of the groundmass glass without a possibility of including a measurement uncertainty (Vermeesch, 2018) and (d) through the global isochron intercept with the secular equilibrium line calculated by IsoplotR (Vermeesch, 2018). (2) On the other hand, a constant U/Th fractionation factor between zircon and melt can be assumed (Boehnke et al., 2016). In this case, the fractionation factor needs to be approximated. Therefore, we additionally calculated the two-point zircon-melt isochron ages with different U/Th fractionation-factors between zircon and melt ($f_{\text{U/Th}}$) by using the model introduced by Boehnke et al. (2016): (a) $f_{\text{U/Th}} = 7$ as suggested by Boehnke et al. (2016), (b) $f_{\text{U/Th}} = 5$ as often this is the assumed value for initial ^{230}Th disequilibrium corrections (Sakata et al., 2017; Guillong et al., 2014), (c) $f_{\text{U/Th}} = 4$ as a reasonable estimate for a rhyolitic composition (Kirkland et al., 2015) and (d) $f_{\text{U/Th}}$ approximated through comparing the median zircon $^{238}\text{U}/^{232}\text{Th}$ with the measured groundmass glass.

Here, we want to point out that the original code by Boehnke et al. (2016) sets negative Monte Carlo-derived isochron-slopes to zero, effectively interpreting them as zero ages. In young systems (<20 ka), this procedure can artificially inflate model ages and bias statistical eruption age estimates. Therefore, to preserve unbiased results, we modified the code to retain negative slopes, and we recommend that others using this approach consider doing the same. While negative slopes are not geologically meaningful, retaining them preserves the statistical integrity and uncertainty structure of the Monte Carlo simulations.



135 2.1.4 U-Pb data Processing

For this study, U–Pb data were processed separately. Very young zircon (<1 Ma) have not accumulated sufficient radiogenic ^{207}Pb to overprint potential common lead signals. This puts more weight on the common lead correction and therefore on the $^{207}\text{Pb}/^{206}\text{Pb}$ ratio. Two primary approaches exist for calculating isotope ratios from LA-ICP-MS data acquired during an ablation interval: the ratio of integrated intensities (ROI) and the mean of individual point-by-point ratios (MOR). They can
 140 diverge significantly when dealing with low-count isotopes such as ^{207}Pb and ^{206}Pb in young zircon (Ogliore et al., 2011). To mitigate the bias introduced by low-count statistics, especially in young and radiogenic Pb-poor zircon, we decided to adopt the ROI method to calculate the isotopic ratios. As the default U–Pb Geochronology DRS in Iolite calculates isotope ratios using the MOR approach (Paton et al., 2010), we developed a custom DRS that first calculates ROI values, and then applies downhole fractionation, a relative sensitivity factor and mass bias corrections to the ablation intervals using the corresponding
 145 time slices of primary reference zircon (Paton et al., 2010). However, this is a simplification and could be improved by adopting statistically or physically more robust methods (Vermeesch, 2022, 2025).

To finally calculate the U–Pb ages of the young volcanic zircon to be later compared with the U–Th ages for the same ablation volumes, we used the DQPB model by Pollard et al. (2023) to retrieve the ^{207}Pb -corrected ages. Initial disequilibrium was corrected through an assumed Th/U fractionation ($D_{\text{Th/U}}$) of 0.2 ± 0.04 between zircon and melt. To correct for common
 150 lead, an intercept of $^{207}\text{Pb}/^{206}\text{Pb} = 0.8356 \pm 0.01$ was used (Stacey and Kramers, 1975).

2.2 Modelling approach for eruption age calculation

2.2.1 Generating synthetic U–Th data

To evaluate the performance of different eruption age approaches, we generated synthetic U–Th age datasets with known eruption ages. We compared the ability of each method to reproduce the eruption ages most accurately and precisely. These synthetic
 155 distributions incorporate the analytical uncertainties (σ), number of zircons (N_{zircon}), and duration of zircon crystallization (Δt) relevant to natural U–Th LA-ICP-MS data.

(1) First, the model must randomly sample zircon dates from an underlying distribution representing the crystallization of zircon between zircon saturation and the eruption. The choice of the underlying distribution is not straightforward, as the crystallization of zircon over time is not constant and depends on the individual temperature history and chemical composition of
 160 the systems (Schmitt et al., 2023). Magmatic zircon crystallization is well studied in terms of empirical saturation equations and kinetic models (Watson and Harrison, 1983; Watson, 1996; Boehnke et al., 2013), and predicts a peak in zircon crystallization at zircon saturation for monotonic cooling. Natural systems are more complex and do not strictly follow these simple temperature histories. Nathwani et al. (2025) demonstrates that zircon distributions from volcanic units tend to skew toward young ages, where crystallization of zircon has been truncated by the eruption, whereas plutonic zircon distributions reflect
 165 the kinetic models more accurately. Therefore, we decided to sample three different distributions to reflect the end members of zircon crystallization in volcanic systems: (i) a truncated normal distribution, (ii) a truncated monotonic cooling model by Keller et al. (2017), and (iii) a uniform distribution. The uniform distribution is the simplest model that provides a geologi-



cally plausible distribution, suggesting relatively constant zircon production throughout the sampled time interval. This can be translated into representing many non-resolvable repeating crystallization blooms (Baudry et al., 2024). The truncations in the other distributions represent the termination of crystallization as a result of the eruption, with the age peak skewing toward the eruption (Nathwani et al., 2025).

(2) After sampling the underlying zircon age distribution, typical uncertainties observed on U-Th zircon LA-ICP-MS datasets are assigned to the individual ages. Due to the inherent nature of the U-Th disequilibrium method, progressively older zircon, as well as zircon with lower U/Th ratios, will have higher uncertainties on their ages. While we can account for the age dependency by assigning higher uncertainties to the older ages, we also allow the uncertainty to spread around a mean value to account for variable U/Th ratios. Although the uncertainties on U-Th ages are not symmetric due to the non-linearity of the age equation, we apply symmetric uncertainties to the synthetic data for simplicity, as done in many publications (e.g. Baudry et al., 2024), model age tools (e.g. IsoplotR, Vermeesch, 2018), and eruption age estimation methods such as the Bayesian method (Keller et al., 2018) and weighted mean calculations. Finally, we add Gaussian noise to each age within a 2σ range of their assigned uncertainty to most accurately reproduce potential U-Th zircon age datasets.

2.2.2 Eruption age calculation methods

The synthetically produced datasets were further used to reproduce the original eruption age underlying the sampled zircon ages using different methods. Two main families of methods were applied: the weighted mean and the likelihood-based Bayesian approach. Both approaches rely on assumptions, where the weighted mean asks for a decision about the zircon age population included for the calculation, and the Bayesian approach asks for a prior distribution of the zircon ages (Fig. 2). While the weighted mean has the inherent assumption that all zircons within the chosen population have crystallized at the time of eruption, the Bayesian approach spells out the assumption of its prior knowledge in the form of the relative age distribution (Baudry et al., 2024). Keller et al. (2018) has shown that for typical U-Pb age datasets, the performance of weighted mean approaches differs depending on the degree of dispersion of the data, while the Bayesian approach is less sensitive to this and is least likely to underestimate the uncertainties of its reported eruption estimate. Here, we test whether similar performance is observed for typical zircon U-Th LA-ICP-MS datasets.

Using our synthetic zircon U-Th LA-ICP-MS datasets, we tested both methods. We applied the following weighted mean (WM) approaches to different sets of zircon age populations. (1) The first approach is the Youngest 10% WM, where only the 10% youngest ages are included in the weighted mean calculation, with the purpose of keeping the proportion of zircon constant while still having a statistically robust population. (2) The second approach is the i-MSWD WM, where the mean squared weighted deviation (MSWD) is calculated iteratively by adding continuously older ages to the population. Afterwards, the youngest population is identified depending on changes in the i-MSWD values, which are estimated visually based on a plot, where jumps in the i-MSWD values indicate the addition of older age populations (Popa et al., 2020). (3) The third approach is the Acceptable MSWD WM, where the population size is defined by the number of zircon at which the i-MSWD gets closest to the accepted value defined by Wendt and Carl (1991). For the Bayesian approach, we choose three different prior distributions: (1) truncated normal distribution, (2) uniform distribution, and (3) bootstrapped distribution, where the kernel



density function of the data itself serves as the prior distribution. Each method was evaluated in terms of its ability to reproduce the correct eruption age (accuracy) and its uncertainty (precision).

3 Results and discussion

205 3.1 U-Th model age calculation

3.1.1 U-Th-Pb data of KPT zircon

The U-Pb ages from KPT predominantly span a crystallization timescale between 170-280 ka, with an average 2σ uncertainty of 20 ky per age. Using a $D_{Th/U} = 0.25$ to correct for initial Th disequilibrium would yield ages roughly 5 ky younger, which is still within the model age uncertainties. About 20% of the measured zircon signals had either common lead concentrations
210 that were too elevated, or excessively high uncertainties on the $^{207}Pb/^{206}Pb$ ratio, which prevented resolving a reliable crystallization age (Fig. S1). The U-Th ages based on the different assumptions and approximations show a rough spread between 140-350 ka, with higher uncertainties on each age compared to the U-Pb ages. For the method, which uses the measured $^{230}Th/^{232}Th$ and $^{238}U/^{232}Th$ activities in the groundmass glass as a constant melt composition, fewer model ages were resolved, as many datapoints gave infinitely high uncertainties. For the different U-Th model age assumptions, individual U-Th
215 and U-Pb ages are generally in good agreement within 2σ uncertainty (Fig. 3). However, IsoplotR U-Th model ages using the measured U/Th ratio in the groundmass glass show less agreement with their corresponding U-Pb ages, due to their lower reported uncertainties.

3.1.2 U-Th model ages based on constant melt or constant $f_{U/Th}$

Overall, there is no significant difference in fit agreement between individual U-Pb ages and differently determined U-Th
220 disequilibrium model ages (constant melt or constant $f_{U/Th}$), which is why we can not recommend one or the other method conclusively (Fig. 3). Assuming a constant fractionation factor ($f_{U/Th}$) permits spatial and temporal heterogeneity in melt composition, which certainly happens in nature. Variations in U/Th ratios of the zircon are then interpreted as originating from this heterogeneity (Boehnke et al., 2016). Conversely, assuming a constant melt composition suggests homogeneity throughout the magma chamber and during zircon crystallization with insignificant changes or fluctuations of the U/Th ratio
225 (Schmitt, 2011). Subsequently, any U/Th variations would either result from variable U and Th partitioning behaviour or through dilution of the signal by mineral inclusions in the zircon. Trace element measurements reveal that many zircon crystals contain inclusions (Burnham, 2020), detectable via elevated La and P (apatite), Ti and Fe (Fe-Ti oxides), or Al and Fe (melt inclusions). Apatite inclusions notably affect the U/Th activity ratio due to their Th affinity (Keller et al., 2022). However, since trace elements can not be measured in the same laser session as the U-Th dating, their presence can only be inferred indirectly
230 through high ^{232}Th counts suggesting apatite inclusions. In such cases, assuming a fixed fractionation factor is incorrect and is more appropriately dealt with in the constant melt composition method.

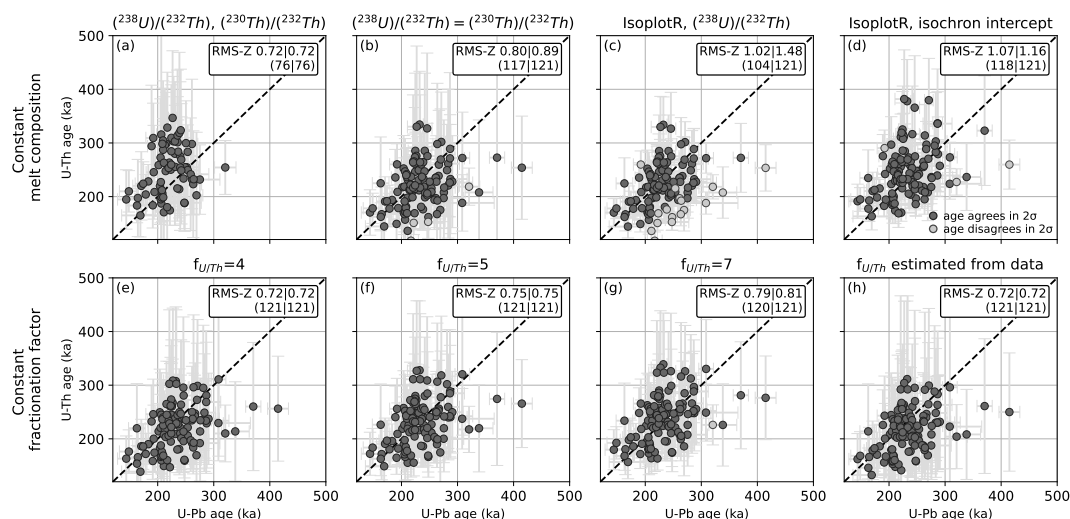


Figure 3. Comparison of KPT U–Pb and U–Th ages from the same ablation volume using different U–Th age calculation approaches. Panels (a)–(d) show U–Th zircon crystallization ages calculated using a constant melt composition, while (e)–(h) use constant U–Th zircon–melt fractionation factors. Dark grey points represent data where U–Th and U–Pb ages agree within 2σ ; light grey points indicate outliers with no overlap. Each panel includes the Root Mean Square of the normalized age difference (RMS-Z) and the number of points considered (overlapping | total). RMS-Z values ≥ 1 indicate decreasing agreement between the U–Th and U–Pb age estimates.

However, the constant melt approach might be questioned when assuming many accessory phases crystallize in boundary layers of other mineral phases, and these get locally enriched in the incompatible elements such as U and Th and may fractionate them, which would change the local melt composition from which the zircon grows. Moreover, on a bigger scale, magmatic systems are rarely homogeneous in space and time (Bachmann and Huber, 2016; Cashman et al., 2017). Melt can be influenced by pre-eruptive mixing processes (e.g. Nakamura, 1995), and zircon datasets show large variations in trace elements (e.g. Troch et al., 2018; Castellanos-Melendez et al., 2024), undermining the assumption of a constant melt composition.

The crystallization of zircon might be even more complicated, as undercooling and disequilibrium growth, which manifests in dendritic growth in zircon can lead to apparent CL growth rims having different U/Th compositions as the corners of the crystal experience fast growth and lower U/Th values, while the later and slower infillings into the planar structures of the zircons have higher U/Th values (Gillespie et al., 2025). This disequilibrium growth mechanism can therefore produce a spread of the U/Th ratio in the zircon without requiring a melt composition change or inclusions, but rather that zircon out of equilibrium is not well described by the bulk partition coefficient (Gillespie et al., 2025). Similarly, sector zoning in zircon has been shown to influence the partitioning of trace elements into zircon greatly within a homogenous melt (Burnham and Berry, 2012; Burnham, 2020). The partitioning behavior of U and Th is further complicated by evolving with melt differentiation (Kirkland et al., 2015) and by U partitioning being dependent on the oxygen fugacity of the system (Burnham and Berry, 2012). All those arguments put doubt on the assumption of constant U/Th fractionation between zircon and melt. This highlights the



complexity of the zircon-melt system and points out that both model age approaches (constant melt vs. constant $f_{U/Th}$) are based on end-member assumptions.

250 3.1.3 Estimating constant melt signature or constant $f_{U/Th}$ for obtaining model ages

Estimating the melt in equilibrium with the crystallizing zircon and defining a representative $f_{U/Th}$ is challenging. Using both measured melt ratios ($^{230}Th/^{232}Th$ and $^{238}U/^{232}Th$) in a zircon-melt isochron approach showed good agreement with U-Pb ages for the KPT zircon (Fig. 3). Yet, high $^{230}Th/^{232}Th$ uncertainties limit the number of resolvable ages. There is an observed scatter in glass $^{230}Th/^{232}Th$ ratios, and minor systematic shifts can significantly influence zircon crystallization ages.

255 Therefore, a more conservative approach assumes the melt is in or close to secular equilibrium, supported by Boehnke et al. (2016). Measuring $^{238}U/^{232}Th$ in the groundmass glass accurately and assuming secular equilibrium, performed best under the constant melt composition models in comparison with the U-Pb ages and is therefore a preferred way of applying the constant melt anchor point. This is similar to the isoplotR calculation with a measured U/Th ratio as a melt anchor, but the measurement uncertainty is propagated. This error propagation has proven important, as many model ages calculated with isoplotR did not
 260 overlap with the U-Pb ages due to uncertainty underestimation (Fig. 3). For the KPT case, using a global isochron intercept performed less well relative to the U-Pb age benchmark than using the measured glass composition.

The constant fractionation models performed equally well compared to the constant melt approach for various fractionation approximations. Among constant fractionation factors, the one using the median zircon signal compared to the measured glass (for KPT: $f_{U/Th} \sim 3.6$) performed well. Using $f_{U/Th} = 7$, as suggested by Boehnke et al. (2016), did not perform as well as the
 265 others, most likely because the $f_{U/Th}$ is overestimated for a rhyolitic system like the KPT (Kirkland et al., 2015). However, given the close match between $f_{U/Th} = 4$ and $f_{U/Th} = 5$ models, and that U-Pb ages were corrected using a $f_{U/Th} = 5$, this appears most suitable and consistent for U-Th age calculations.

Importantly, for older zircon, changing the constant melt composition, as well as a change in the constant fractionation factor, is less significant compared to young zircon with the same analytical uncertainty (Fig. S2). This is potentially the reason
 270 for not seeing distinct differences in the KPT crystals, either for different constant melt assumptions or for different constant fractionation factors. Therefore, we applied different model age methods to younger samples with well-defined eruption ages to validate the findings made based on the KPT zircon.

3.1.4 Young isochron intercept to validate U-Th model ages

The Japanese sample, Heisei, from the historic eruption at Unzen volcano, illustrates that measured groundmass glass compositions may not reliably reflect the zircon-forming melt. The zircon crystals show prolonged crystallization, by plotting into
 275 a wedge-shaped field forming an almost perfect spheonochron (Fig. 4a). About 9% of the datapoints show strongly enhanced ^{232}Th counts, suggesting influence of apatite inclusions. No measurement falls below a $(^{230}Th)/(^{232}Th)$ activity ratio of ~ 1.5 , while in the groundmass glass activity ratios of $(^{238}U)/(^{232}Th) = 0.684 \pm 0.006$ and $(^{230}Th)/(^{232}Th) = 0.66 \pm 0.08$ have been measured. Even the youngest calculated model ages using the measured groundmass glass either as a constant melt anchor
 280 point or to estimate the fractionation factor fall well above the eruption age (Fig. 4b). There is no evidence for zircon resorp-

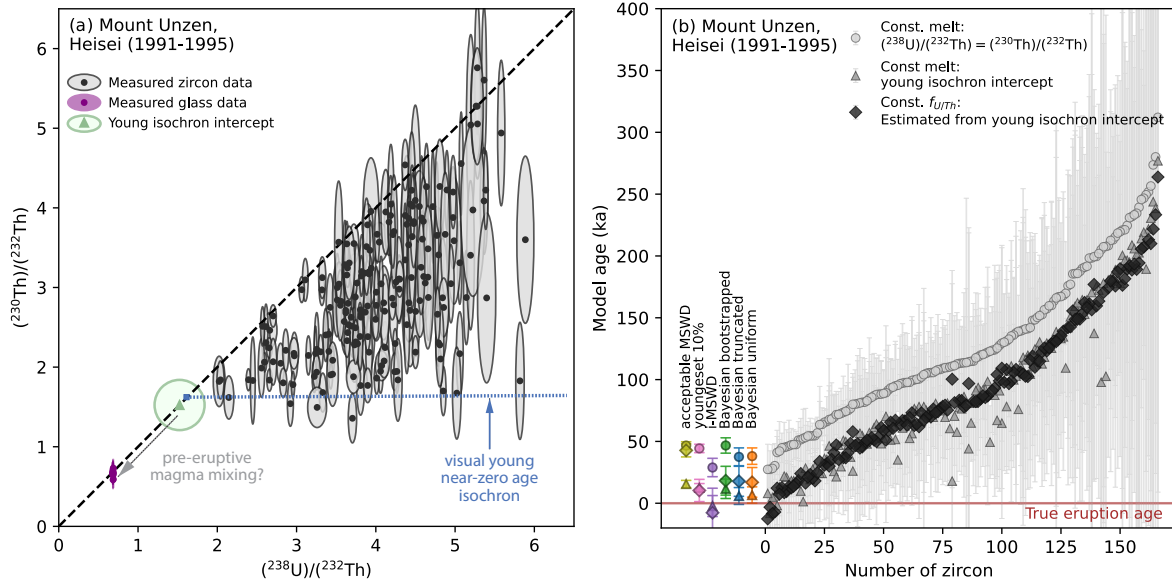


Figure 4. Validation of U–Th zircon age determinations using the Heisei sample from the 1991–1995 Unzen eruption. (a) U–Th evolution plot showing measured zircon and groundmass glass activity ratios, the young isochron intercept evaluated using IsoplotR (Vermeesch, 2018), and the visually identified young near-zero age isochron. The discrepancy between the measured groundmass glass and the young isochron intercept indicates that the groundmass glass does not represent the melt from which the zircon crystallized. (b) Zircon crystallization ages and eruption age estimates for the Heisei sample were calculated using different approaches.

tion that could explain this gap between the eruption age and the latest recorded zircon crystallization. A visual assessment of the evolution plot shows that the low- $(^{230}\text{Th})/(^{232}\text{Th})$ datapoints form an almost horizontal array, consistent with a young near-zero-age isochron for this historic sample. However, this young isochron intercepts the secular equilibrium line significantly above the measured groundmass glass. This is a strong indication that, for this sample, the fresh and microlite-rich groundmass glass (Noguchi et al., 2008) is not representative of the melt from which the zircon crystallized. Since this eruption was strongly influenced by immediately pre- and syn-eruptive mixing between resident silicic, zircon-bearing mush in the upper crust, and more mafic recharge coming from deeper in the system (Nakamura, 1995), it is likely that the melt changed its composition significantly and is no longer in equilibrium with any of the zircons from this sample. A possible solution to this issue is to estimate the melt composition through fitting a young isochron over the spheonochron and using its intercept with the secular equilibrium line as a constant melt anchor point. To estimate the young isochron intercept, we applied a workflow of calculating the isochron of the whole dataset using isoplotR (Vermeesch, 2018) and iteratively removing the oldest ages and recalculating the isochron until the MSWD reaches a value of 1. From there, we retrieved the young isochron intercept. For this Heisei sample, this approach suggested an intercept of 1.52 ± 0.32 (2σ). By using this intercept as a melt anchor point to calculate the model ages, the crystallization timescale of this sample is more accurately represented, as the youngest crystallization ages overlap with the known eruption age. Estimating the $f_{U/Th}$ through the isochron intercept of 2.7 also yielded more appropriate

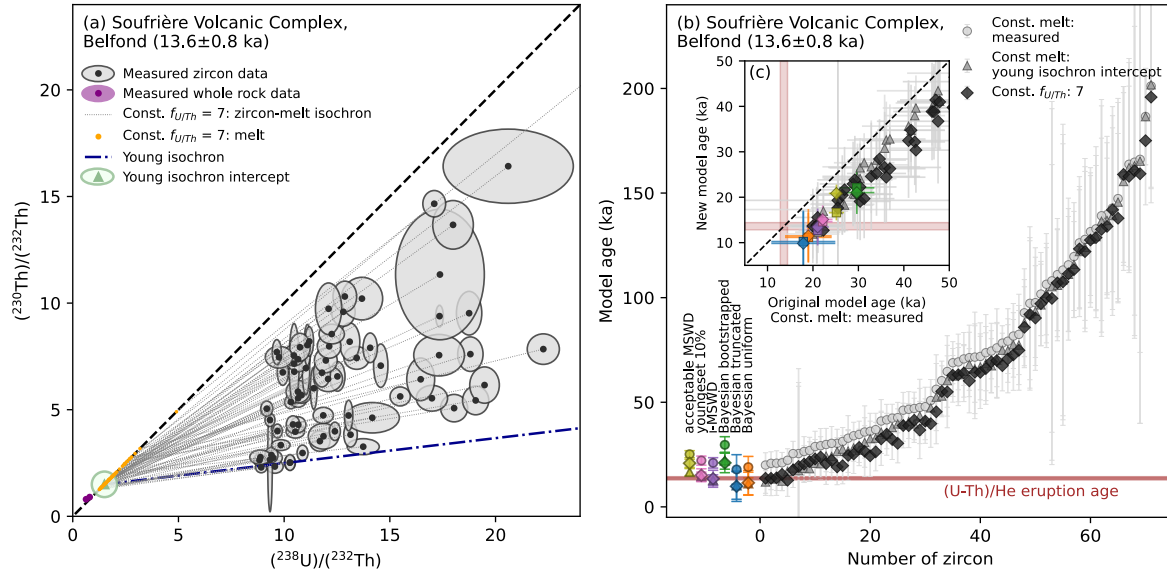


Figure 5. Literature-based zircon U–Th data from Belfond Dome (SL-25, SL-51) used as a second validation case study. (a) U–Th evolution plot showing published zircon activity ratios (Schmitt et al., 2010) and the whole-rock composition (Turner et al., 1996). Two-point zircon–melt isochrons were estimated using a constant $f_{U/Th} = 7$, as suggested by Boehnke et al. (2016), showing the range of resulting melt compositions (orange) and a potential young isochron with its intercept at 1.5 ± 0.6 . The discrepancy between the whole-rock composition and the young isochron intercept suggests that the whole rock is not representative of the melt from which the zircon crystallized. (b) Zircon crystallization ages calculated using three approaches and eruption age estimates, with a close-up for the youngest crystallization ages in (c): the originally published ages using the constant whole-rock melt composition (Schmitt et al., 2010), a constant $f_{U/Th}$ of 7 (Boehnke et al., 2016), and a new constant melt approach of using the young isochron intercept. Eruption age estimates are compared to the (U–Th)/He eruption age of 13.8 ± 0.8 ka (Schmitt et al., 2010).

crystallization ages. However, as this sample is strongly influenced by apatite inclusions, the assumption of a constant $f_{U/Th}$ becomes increasingly difficult to justify. Therefore, for this sample, we suggest calculating the crystallization ages through a constant melt approach by using the young isochron intercept as a melt anchor point.

Similarly, for the Belfond dome, using the whole rock composition, $(^{230}\text{Th})/(^{232}\text{Th}) = 0.85 \pm 0.07$ and $(^{238}\text{U})/(^{232}\text{Th}) = 0.72 \pm 0.12$ (Turner et al., 1996), as a constant melt anchor point is overestimating its zircon crystallization ages (Boehnke et al., 2016), assuming no resorption took place and zircon crystallized until eruption (Schmitt et al., 2010). Boehnke et al. (2016) has shown that calculating the crystallization ages using a constant $f_{U/Th}$ of 7 more accurately aligns with the proposed eruption age of 13.6 ± 0.8 ka (Schmitt, 2011). Using a young isochron intercept of 1.5 ± 0.6 , which notably does not overlap with the measured whole rock signature (Fig. 5a), as a constant melt anchor point, results in very similar crystallization ages compared to using a constant $f_{U/Th}$ of 7 (Figure 5b,c).

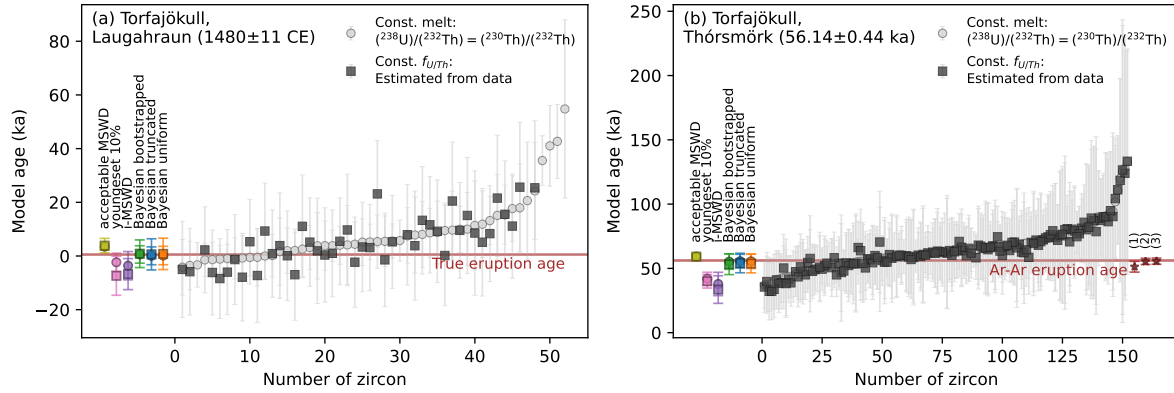


Figure 6. Zircon crystallization and eruption age estimates for two validation samples from the Torfajökull volcanic system, Iceland. (a–b) Zircon crystallization ages and eruption age estimates for two samples from Torfajökull, shown alongside suggested eruption ages for Laugahraun based on teprochronology (Larsen, 1984) and the most recently published Ar-Ar age of glassy fiamme from the Thórsmörk ignimbrite (Groen and Storey, 2022). Additional independent eruption age estimates for Thórsmörk are indicated on the left: (1) Moles et al. (2019), (2) Svensson et al. (2008), (3) Guillou et al. (2019).

The Icelandic samples, Laugahraun (LH) and Thórsmörk (TH), do not show very prolonged crystallization but rather restricted spheochrones. The young isochron intercept at 1.05 ± 0.2 for LH and 1.18 ± 0.4 for TH overlap with their corresponding groundmass glass signatures: $(^{238}\text{U})/(^{232}\text{Th}) = 0.968 \pm 0.006$ and 0.97 ± 0.06 , $(^{230}\text{Th})/(^{232}\text{Th}) = 1.03 \pm 0.12$ and 0.97 ± 0.12 , for LH and TH respectively. This suggests that the melt from which the zircon grew is well represented by the groundmass glass. Apatite inclusions are evident in about 6% of the isotopic signals based on enhanced Th concentrations. Model ages calculated with the constant melt approach of using the measured $(^{238}\text{U})/(^{232}\text{Th})$ in the groundmass glass and assuming secular equilibrium are similar within uncertainty to the model ages using a constant $f_{\text{U/Th}}$ approximated by the median zircon U/Th and groundmass glass U/Th of 3.8 and 5.8, for LH and Th respectively (Fig. 6).

In contrast to Boehnke et al. (2016), we emphasize that using whole rock or groundmass glass as a constant melt anchor point does not generally overestimate ages. However, if the whole rock or groundmass glass is not representative of the melt, as for the Japanese and the Belford Dome sample, then the model ages will be inaccurate. An inappropriate $f_{\text{U/Th}}$ can also bias the model ages, either too old for high $f_{\text{U/Th}}$ or too young for low $f_{\text{U/Th}}$. Therefore, both methods depend heavily on accurate estimations of either equilibrium melt composition or average $f_{\text{U/Th}}$.

3.1.5 Recommendations for calculating U-Th model ages

Following the discussion and investigation of the KPT data, as well as the evaluation of the Icelandic and Japanese samples, we can make suggestions on how to retrieve the most reliable zircon crystallization ages from U-Th data. For the constant melt approach, in a first step, the reliability of the measured groundmass glass or whole rock data should be assessed. If a young isochron intercept does not overlap within the uncertainty of the measured glass composition, this suggests that the measured



glass is not representative of the melt and should not be used as an anchor point. An alternative method would then be to use
 325 the young isochron intercept itself as an anchor point. However, if it overlaps the measured glass composition, this gives more
 confidence that the glass composition represents the equilibrium melt.

In terms of estimating a constant $f_{U/Th}$, we propose a combination of an initial value assessed for the system (based on
 literature values, direct measurements, chemistry of the system, tuning sample with known eruption age) and approximating
 it by using the median zircon signal with the appropriate melt value. This should yield a reasonable estimate for a constant
 330 $f_{U/Th}$.

As we have discussed, both approaches represent endmember cases, but for reasonable estimations of the constant equilib-
 rium melt composition or $f_{U/Th}$, the overall model age spectra should be similar and comparable. However, using a constant
 fractionation factor on a zircon with a strong apatite signal will overestimate its age. Measurements with exceptionally high
 Th counts or unreasonably low U/Th ratios, evident from Iolite output, should ideally be excluded, as they bias statistical age
 335 estimates.

3.2 Eruption age estimate using U-Th crystallization ages

3.2.1 Accuracy and precision of different eruption age estimate approaches

To evaluate the eruption estimate approaches, accuracy and precision for each method were compared. Here we define the
 accuracy as the difference between the estimated and true (synthetic) eruption age, while precision is defined as the 2σ un-
 340 certainty of the estimated eruption age. We also compare whether the reported uncertainty is realistic relative to the given
 accuracy, using the percentage of how often the true eruption age falls within the 2σ uncertainty of the eruption estimate (Fig.
 7).

By comparing these parameters across different approaches, several interesting observations can be made for the two age
 ranges we simulated (0–40 ka and 55–170 ka) and as a function of N_{zircon} (10, 30, 50, 70, 90, 110, 130, 150). The accuracy
 345 of the eruption age estimates generally increases with N_{zircon} . However, for the acceptable MSWD WM the accuracy stagnates
 at a comparable high deviation from the true eruption age, while the i-MSWD WM typically overestimates the eruption age
 for low N_{zircon} while underestimating it for high N_{zircon} . The best and most consistent accuracy is achieved by the Bayesian
 approach with the truncated normal or the uniform prior distribution, shortly followed by the bootstrapped prior distribution
 and the youngest 10% WM approach. As expected, the accuracy and the precision of all eruption age estimates are better for
 350 the young eruption ages than for the older ones, due to lower uncertainties of the underlying data. The precision increases for
 increasing N_{zircon} for all approaches, except for the i-MSWD approach, which plateaus at a lower N_{zircon} . The weighted mean
 approaches tend to underestimate the uncertainty, yielding poorer confidence in the eruption ages. This is most significant for
 the acceptable MSWD WM, as it only captures about 2% of the eruption ages, while the i-MSWD WM retrieves the eruption
 age in 73% of the cases. Best and most consistent performance of the weighted mean approaches across the range of N_{zircon} was
 355 yielded by the 10% youngest zircon with a confidence of 89%. Generally, Bayesian approaches tend to capture the uncertainty
 more adequately. The prior uniform distribution and the truncated normal distribution perform best and most steadily with

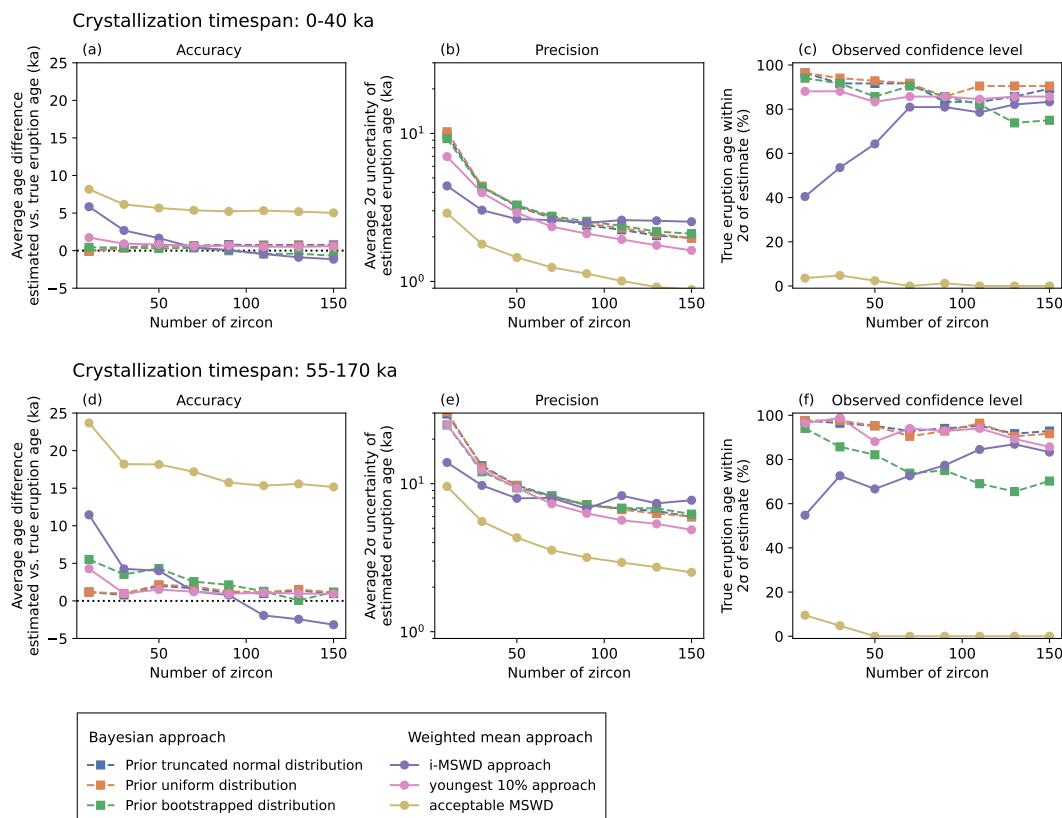


Figure 7. Accuracy and precision of different eruption age estimation approaches as a function of the number of zircons and two crystallization timescales: (a–c) 0–40 ka and (d–f) 55–170 ka. (a) and (d) Accuracy, expressed as the average difference between the estimated and true eruption ages, with the ideal value of zero indicated by a black dotted line. (b) and (e) Precision, shown as the average 2σ uncertainty of each method. (c) and (f) Percentage of cases where the true eruption age falls within the 2σ uncertainty of the estimate.

high levels of observed confidence of averaging 93% and 92% respectively, while the bootstrapped prior distribution only retrieved 81% of the eruption ages. There is no significant difference in the performance of the truncated normal or uniform prior distribution in the Bayesian approach as a function of the underlying sampled distribution, which would suggest any bias in favor of the tested prior distributions compared to the weighted mean approaches.

3.2.2 Optimal approach to estimating eruption ages using zircon U-Th data

Our results indicate that Bayesian approaches (with uniform and truncated normal distributions as priors) are the best-performing methods for calculating eruption ages using low-dispersed U-Th data, while the WM approaches are not satisfactory, similar to the findings of Keller et al. (2018) and Baudry et al. (2024).



365 The acceptable MSWD WM approach fails to accurately predict the eruption age, which is inherent in the choice of simulating continuous ages within a rather extended timeframe and global MSWDs of mainly 2.5 and higher. It has been shown that those approaches overestimate the eruption age significantly for prolonged and continuous crystallization (Keller et al., 2018). Furthermore, given the increasing number of zircon ages, the uncertainty of the method decreases as it is inversely proportional to the root of the number of samples, which draws a false picture by increasing confidence.

370 The i-MSWD WM approach also performed unsatisfactorily. At low N_{zircon} , the i-MSWD method tends to overestimate the eruption age, while for high N_{zircon} , it tends to underestimate it. This effect is linked to the relative size of the selected youngest zircon population. With fewer zircons, the proportion of zircon to cause a detectable MSWD jump must be larger, skewing the age estimate older. Conversely, with larger datasets, smaller proportions or ages suffice, often biasing the estimate to younger ages. In the specific case of our synthetic dataset, no distinct young population was implemented, but rather continuous crystallization, similar to what can be resolved in natural datasets for U-Th data. Given the high uncertainties of typical U-Th LA-ICP-MS zircon ages, true young zircon populations are most likely overprinted by Gaussian noise and are unlikely to be resolved. In our synthetic data, any MSWD jumps are randomly generated by Gaussian noise and the given uncertainties and do not reflect underlying geological signals. These jumps are often driven by low uncertainty dates, not by the presence of distinct zircon age populations. Therefore, in the absence of a clear population structure visible in the age plot, visual jumps
 375 in the iteratively calculated MSWD are arbitrary and not significant, and influenced by analytical artifacts rather than true geological signals. Because the selection is based on visually identified and often ambiguous MSWD changes, this approach lacks the objectivity and reproducibility necessary for robust eruption age estimation, particularly in low-dispersed datasets.

The WM approach, which seemingly performed best and most consistently for our simulated timescales, was the weighted mean of the 10% youngest zircon ages. The general idea was to use a constant proportion of young zircon ages to respect the
 385 statistical need to base the eruption age on multiple data points rather than based on the youngest zircon age alone as well as assuming that the eruption age is best reflected by the young population, while being objective enough to include a constant proportion of the sampled data to avoid systematic shifts. However, here we have only assessed two specific timescales with different levels of uncertainty, which by chance are well described by a WM of the 10% youngest zircon. If the crystallization timescale is shorter and inherently the dispersion gets lower, the best constant percentage will inevitably change towards higher proportions, with an endmember case of instantaneous crystallization allowing for a justified global weighted mean approach, while the opposite is true for increasing dispersion (Fig. S3). This illustrates that using a constant proportion of zircon for a
 390 weighted mean approach is too sensitive to the dispersion of the dataset and therefore will perform inconsistently.

In contrast to the weighted mean (WM) approaches, which implicitly assume that the selected zircon population represents one single crystallization age (Baudry et al., 2024), the Bayesian approach takes into account the entire zircon crystallization
 395 dataset with its uncertainties. It still requires an explicit assumption of the underlying age distribution to inform the eruption age calculation. However, as this is in better accordance with true zircon crystallisation in a dynamic magmatic system (Schmitt et al., 2023), we prefer the Bayesian over the weighted mean methods.

Previous work (Keller et al., 2018) and our study indicate that the choice of prior can affect the accuracy of the calculated eruption age, but not dramatically for reasonably well-constrained priors that capture the general shape of the underlying



400 zircon crystallization age distribution. Investigation of the most suitable prior for high precision zircon U-Pb datasets suggests a bootstrapped prior to be best suitable for well-resolved age dispersion, while a uniform prior is more applicable to low-MSWD datasets (Keller et al., 2018). As expected, for our low-dispersed datasets, the bootstrapped distribution did not perform best. This is likely partially driven by the increasing uncertainties towards older ages for U-Th datasets, as this inherently distorts the bootstrapping and will not represent an underlying zircon crystallization distribution (Fig. S4). This distortion effect is stronger
 405 in the modelled crystallization period of 55-170 ka, explaining why the performance of the bootstrapped prior was poorer for this crystallization period compared to 0-40 ka.

Our analysis shows that both uniform and truncated normal priors perform equally well for U-Th datasets and are useful for retrieving eruption ages. Since most volcanic zircon crystallization is truncated by eruption (Nathwani et al., 2025), a truncated normal prior is reasonable. However, because U-Th uncertainties increase toward older ages, even a dataset drawn
 410 from a uniform distribution naturally approximates a truncated normal shape (Fig. S4). With the relatively high uncertainties of U-Th LA-ICP-MS dating, a uniform prior makes fewer assumptions and best reflects periodic zircon growth, where short growth episodes are overprinted by age uncertainties (Fig. S4). We therefore prefer the uniform distribution for volcanic U-Th datasets, in agreement with Baudry et al. (2024).

3.2.3 Eruption age estimates of validation samples

415 The different eruption age estimate approaches were also applied to the three natural samples from Japan and Iceland with known eruption ages (Fig. 6). The acceptable MSWD WM overestimates the eruption age for all three samples. For the Icelandic samples, where the crystallization period is shorter and the ages are less dispersed, the 10% youngest WM underestimates the true eruption age, while overestimating it for the strongly dispersed Japanese sample. This highlights that the weighted mean approaches are strongly affected by the dispersion of the data (Fig. S3). The i-MSWD approach strongly underestimates the
 420 eruption age of the Thórsmörk sample, but approaches the true eruption age of the other two samples. In accordance with the results from the synthetic datasets, the Bayesian method using the truncated normal and the uniform distribution behaved most consistently. The eruption ages of the Icelandic samples were retrieved, while the eruption age of the Japanese sample is within the uncertainty of the truncated normal Bayesian eruption estimate. A reason for slightly overestimating the eruption age is most likely related to the model age calculation rather than the eruption estimate approach. A young isochron intercept slightly
 425 higher of 1.6 ± 0.4 (2σ) rather than using 1.52 ± 0.32 (2σ) retrieved through the workflow described above, would lower the Bayesian eruption estimates by ~ 4 ka, more accurately retrieving the true eruption age.

3.3 U-Th-Pb double-dating

3.3.1 U-Th and U-Pb double-dating of the KPT zircon

By estimating the eruption age of the KPT sample with our preferred eruption age method (truncated normal or uniform
 430 Bayesian) for the most agreeable U-Th model age approaches relative to the U-Pb ages (constant melt with secular equilibrium assumption and constant $f_{U/Th}$ of 5), we can test the applicability of our new U-Th-Pb method. The U-Th model ages of the

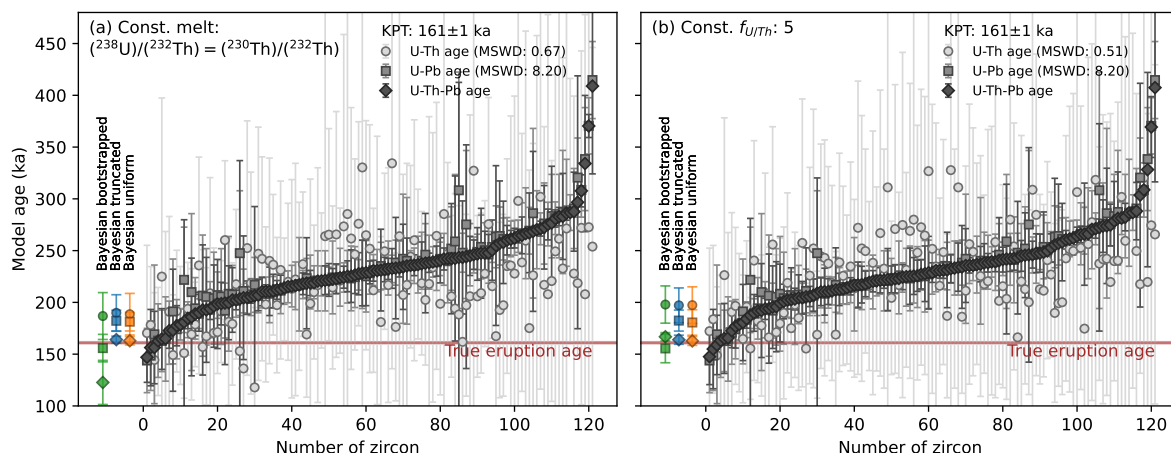


Figure 8. Overview of uniform and truncated normal Bayesian eruption age estimates for the KPT data, compared to the published eruption age of 161 ± 1 ka (Smith et al., 1996). (a) U-Th model ages calculated using the constant melt approach by measuring $(^{238}\text{U})/(^{232}\text{Th})$ and assuming secular equilibrium. (b) U-Th model ages calculated using a constant fractionation factor ($f_{\text{U/Th}} = 5$). Only zircon data with overlapping U-Th and U-Pb ages within 2σ were included. The combined U-Th-Pb ages represent individually weighted mean ages of the overlapping U-Th and U-Pb ages.

KPT, with a crystallization tail between 160-300 ka, have high individual uncertainties, and the MSWD falls well below 1 (Fig. 8). As a result, the Bayesian approach fails to recover the published eruption age of 161 ka (Smith et al., 1996), instead converging toward the weighted mean age. These high uncertainties obscure the true crystallization distribution and ultimately limit the resolution of the eruption age. Interestingly, the eruption age is also overestimated when using only U–Pb ages, despite the greater age dispersion and a high MSWD of 8.2. This likely reflects the challenges of resolving crystallization ages for the youngest zircons in the U–Pb system, where uncertainties increase due to low radiogenic Pb and the greater influence of common lead corrections. By evaluating both the U–Th and U–Pb ages from the same ablation volume and calculating a weighted mean U–Th–Pb age for each zircon, greater emphasis is placed on crystals with internally consistent ages. This results in a more robust and well-constrained crystallization age spectrum. Using this combined dataset, the Bayesian method with a uniform or truncated normal prior distribution successfully retrieves the published eruption age of 161 ka within uncertainty for the KPT sample.

3.3.2 Applicability of the new U-Th-Pb dating routine

The newly presented method for LA-ICP-MS of simultaneous measurement of U-Th-Pb on zircon works well in resolving U-Th disequilibrium and U-Pb age for the period between roughly 150-300 ka. Within this timeframe, both methods reach their limits. However, with this approach and the two independent ages, more confidence in their crystallization age can be achieved. On one hand, for younger zircons, the U-Pb age will have increasingly more difficulties resolving the crystallization ages, especially

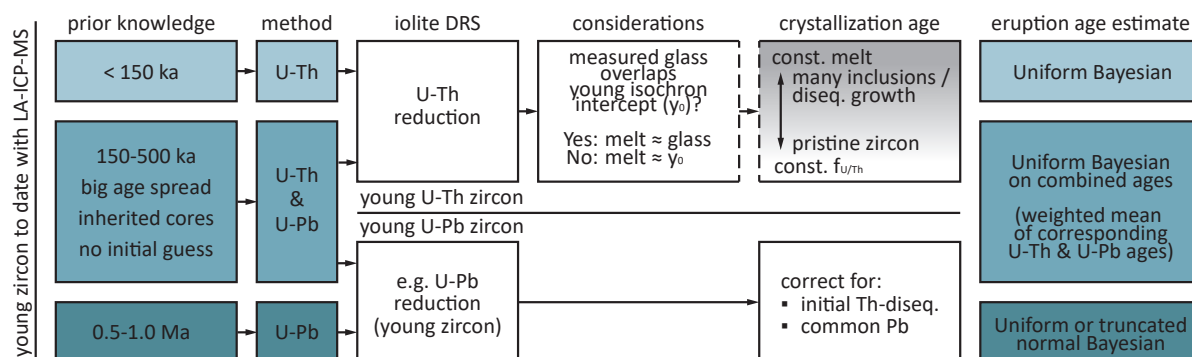


Figure 9. Proposed workflow to date young zircon (<1 Ma) and outline of the applicability of the newly presented U-Th-Pb double-dating method. The time ranges for different dating approaches are specified, along with the custom ionite DRS that can be applied. The favorable method of determining individual zircon crystallization ages is described, including the crucial assessment of whether the measured groundmass glass signal overlaps with the young isochron intercept to evaluate the reliability of the groundmass glass measurement. Finally, the recommended method for estimating the eruption age is provided.

if the zircons are U-poor. However, in this case, the U-Th ages should gain confidence, as they diverge further from secular equilibrium. On the other hand, for older zircon crystals already in secular equilibrium, the U-Pb age gets increasingly better, as more of the radiogenic Pb will reduce the impact of the common lead correction, subsequently inducing more confidence in the U-Pb ages. Therefore, for samples with crystallization ages younger than 150 ka, we suggest using the classic U-Th dating method (Guillong et al., 2016), as the dwell time on ^{230}Th is higher and therefore better resolution on the U-Th age can be achieved, especially if the samples are young or U-poor and small amounts of ^{230}Th have been produced. However, if the samples are older than 150 ka, without knowing the exact age range, or if the samples frequently contain inherited and recycled cores, this new method can add confidence for the younger crystals (via U-Th or combined U-Th and U-Pb ages), while also providing ages for older crystals and their inherited cores via U-Pb (Fig. 9).

3.4 Outlook

Significant progress has been made in recent decades toward refining geochronological strategies for young zircon (Guillong et al., 2014; Sakata et al., 2017), particularly in calculating and interpreting crystallization ages and translating them into eruption age estimates (Schmitt, 2011; Boehnke et al., 2016; Keller et al., 2018). This study contributes to that ongoing development, while also highlighting several key areas where methodological improvements are still needed. In particular, more statistically robust approaches for handling low-count or zero-count signals in isotopic measurements could enhance the reliability of crystallization age determinations. For U-Th model ages, developing a generalizable framework that interpolates between the endmember assumptions of constant melt composition and constant fractionation factor, applicable across diverse sample types, would represent a major advance. A critical component of such a framework would be the accurate and robust estimation of young isochron intercepts based on sample activity ratios to better evaluate the representability of the measured



groundmass glass. An alternative way to justify the constant $f_{U/Th}$ endmember approach could be to remove glass and apatite inclusions from zircon crystals by acid washing prior to analysis. Additionally, the asymmetric nature of uncertainties in U–Th model ages should be better addressed; representing them symmetrically misrepresents the true error structure. While Bayesian approaches currently require symmetric uncertainties, using isochron-slopes (rather than ages) as model input provides a promising alternative, as these can be characterized by symmetric errors. However, this shift would also necessitate revisiting prior distributions, as the resulting slope distributions are of a different form than the age distribution and are further dependent on the crystallization timescale (Fig. S5).

4 Conclusions

The U–Th–Pb double dating of the KPT zircons and the samples from Iceland and Japan have shown that for reasonable estimates of either the melt composition or the fractionation factor, individual crystallization ages can diverge, but the overall crystallization age spectra look similar. However, in the case of a strong influence of apatite inclusions and evidence of disequilibrium growth, the constant melt anchor point method is preferred.

Furthermore, we validated the application of Bayesian eruption age estimates and weighted mean approaches for U–Th datasets, which are characterized by increasing uncertainties towards older ages. As the performance of weighted mean approaches is highly dependent on the dispersion of the data, we prefer the Bayesian method as it provides superior accuracy and estimates of uncertainties in most cases. Given the typical high individual uncertainties involved in the LA–ICP–MS dates, we recommend the use of a uniform prior distribution to estimate eruption ages from U–Th zircon datasets.

The combined U–Th–Pb dating strategy of LA–ICP–MS measurements can be applied to any young volcanic zircon below roughly 1 Ma. The U–Th ages can be resolved up to ~300 ka, and U–Pb from ~150 ka onwards, depending on the U content. Consequently, this allows us to gain more confidence in the overlapping period of 150–300 ka, which covers the respective limits of both U–Th and U–Pb dating. Additionally, the ages of inherited cores of young zircon can be retrieved, which would otherwise be hidden by secular equilibrium.

Code and data availability. The code and data used in this study are openly available at Zenodo: <https://doi.org/10.5281/zenodo.16926790> (Moser, 2025). The repository contains a Python-based Bayesian eruption age estimation function, custom Iolite data reduction schemes, the synthetic U–Th data generator, and a data file containing the LA–ICP–MS data, the calculated model ages, and eruption age estimates.

Author contributions. Conceptualisation: ZM, MG, CN, OB. Data curation: ZM, KI. Formal analysis: ZM. Software: ZM, MG, CN. Investigation: ZM, MG. Methodology: ZM, MG. Resources: OB. Writing (original draft preparation): ZM. Writing (review and editing): MG, CN, KI, RGP, OB.



495 *Competing interests.* The authors declare no conflicts of interest related to this work. We have no commercial or financial relationships that could be construed as a potential conflict of interest.

Acknowledgements. This work was supported by the Swiss National Science Foundation (grant 214930). Thanks to Iolite for providing a free student licence. We thank Sæmundur Ari Halldórsson and Kristján Jónasson for their contributions during the fieldwork in Iceland. We thank Dawid Szymanowski and Francesca Forni for helpful discussions.



500 References

- Bachmann, O.: Timescales Associated with Large Silicic Magma Bodies, in: Timescales of Magmatic Processes: From Core to Atmosphere, edited by Bosseto, A., Turner, S. P., and Van Orman, J. A., 2010.
- Bachmann, O. and Huber, C.: Silicic magma reservoirs in the Earth's crust, *American Mineralogist*, 101, 2377–2404, <https://doi.org/10.2138/am-2016-5675>, 2016.
- 505 Bachmann, O., Charlier, B. L., and Lowenstern, J. B.: Zircon crystallization and recycling in the magma chamber of the rhyolitic Kos Plateau Tuff (Aegean arc), *Geology*, 35, 73–76, <https://doi.org/10.1130/G23151A.1>, 2007a.
- Bachmann, O., Oberli, F., Dungan, M. A., Meier, M., Mundil, R., and Fischer, H.: 40Ar/39Ar and U-Pb dating of the Fish Canyon magmatic system, San Juan Volcanic field, Colorado: Evidence for an extended crystallization history, *Chemical Geology*, 236, 134–166, <https://doi.org/10.1016/j.chemgeo.2006.09.005>, 2007b.
- 510 Baudry, A., Singer, B. S., Jicha, B., Jilly-Rehak, C. E., Vazquez, J. A., and Keller, C. B.: A Bayesian age from dispersed plagioclase and zircon dates in the Los Chocoyos ash, Central America, *Earth and Planetary Science Letters*, 643, <https://doi.org/10.1016/j.epsl.2024.118826>, 2024.
- Björke, J. K.: Fluid-rhyolite interaction in geothermal systems, Torfajökull Iceland - secondary surface mineralogy and fluid chemistry upon phase segregation and fluid mixing, Master's thesis, University of Iceland, Reykjavík, Iceland, <http://hdl.handle.net/1946/5534>, 2010.
- 515 Boehnke, P., Watson, E. B., Trail, D., Harrison, T. M., and Schmitt, A. K.: Zircon saturation re-revisited, *Chemical Geology*, 351, 324–334, <https://doi.org/10.1016/j.chemgeo.2013.05.028>, 2013.
- Boehnke, P., Barboni, M., and Bell, E. A.: Zircon U/Th model ages in the presence of melt heterogeneity, *Quaternary Geochronology*, 34, 69–74, <https://doi.org/10.1016/j.quageo.2016.03.005>, 2016.
- Burnham, A. D.: Key concepts in interpreting the concentrations of the rare earth elements in zircon, *Chemical Geology*, 551, <https://doi.org/10.1016/j.chemgeo.2020.119765>, 2020.
- 520 Burnham, A. D. and Berry, A. J.: An experimental study of trace element partitioning between zircon and melt as a function of oxygen fugacity, *Geochimica et Cosmochimica Acta*, 95, 196–212, <https://doi.org/10.1016/j.gca.2012.07.034>, 2012.
- Cashman, K. V., Sparks, R. S. J., and Blundy, J. D.: Vertically extensive and unstable magmatic systems: A unified view of igneous processes, *Science*, 355, <https://doi.org/10.1126/science.aag3055>, 2017.
- 525 Castellanos-Melendez, M. P., Dilles, J., Guillong, M., Bachmann, O., and Chelle-Michou, C.: From birth to death: The role of upper-crustal thermal maturation and volcanism in porphyry ore formation revealed in the Yerington district, *Earth and Planetary Science Letters*, 647, <https://doi.org/10.1016/j.epsl.2024.119053>, 2024.
- Cisneros de León, A., Danišík, M., Schmitt, A. K., Schindlbeck-Belo, J. C., Kutterolf, S., Mittal, T., Garrison, J. M., and Sims, K. W.: Refining the Eruption Chronology of Atitlán Caldera Through Zircon Double-Dating, *Geochemistry, Geophysics, Geosystems*, 26, <https://doi.org/10.1029/2024GC011953>, 2025.
- 530 Coombs, M. L. and Vazquez, J. A.: Cogenetic late Pleistocene rhyolite and cumulate diorites from Augustine Volcano revealed by SIMS 238U-230Th dating of zircon, and implications for silicic magma generation by extraction from mush, *Geochemistry, Geophysics, Geosystems*, 15, 4846–4865, <https://doi.org/10.1002/2014GC005589>, 2014.
- Costa, F.: Chapter 1 Residence Times of Silicic Magmas Associated with Calderas, [https://doi.org/10.1016/S1871-644X\(07\)00001-0](https://doi.org/10.1016/S1871-644X(07)00001-0), 2008.
- 535 Fournier, R. O.: Geochemistry and Dynamics of the Yellowstone National Park Hydrothermal System, *Annual Review of Earth and Planetary Sciences*, 17, 13–53, <https://doi.org/10.1146/annurev.earth.17.050189.000305>, 1989.



- Friedrichs, B., Atıcı, G., Danišák, M., Atakay, E., Çobankaya, M., Harvey, J. C., Yurteri, E., and Schmitt, A. K.: Late Pleistocene eruptive recurrence in the post-collisional Mt. Hasan stratovolcanic complex (Central Anatolia) revealed by zircon double-dating, *Journal of Volcanology and Geothermal Research*, 404, <https://doi.org/10.1016/j.jvolgeores.2020.107007>, 2020.
- 540 Gillespie, J., Klein, B. Z., Moore, J., Müntener, O., and Baumgartner, L. P.: A dendritic growth mechanism for producing oscillatory zoning in igneous zircon, *Geology*, 53, 171–175, <https://doi.org/10.1130/g52641.1>, 2025.
- Groen, M. and Storey, M.: An astronomically calibrated $40\text{Ar}/39\text{Ar}$ age for the North Atlantic Z2 Ash: Implications for the Greenland ice core timescale, *Quaternary Science Reviews*, 293, <https://doi.org/10.1016/j.quascirev.2022.107526>, 2022.
- Guillong, M., Von Quadt, A., Sakata, S., Peytcheva, I., and Bachmann, O.: LA-ICP-MS Pb-U dating of young zircons from the Kos-Nisyros volcanic centre, SE Aegean arc, *Journal of Analytical Atomic Spectrometry*, 29, 963–970, <https://doi.org/10.1039/c4ja00009a>, 2014.
- 545 Guillong, M., Sliwinski, J. T., Schmitt, A., Forni, F., and Bachmann, O.: U-Th Zircon Dating by Laser Ablation Single Collector Inductively Coupled Plasma-Mass Spectrometry (LA-ICP-MS), *Geostandards and Geoanalytical Research*, 40, 377–387, <https://doi.org/10.1111/j.1751-908X.2016.00396.x>, 2016.
- Guillou, H., Scao, V., Nomade, S., Van Vliet-Lanoë, B., Liorzou, C., and Guðmundsson, A.: $40\text{Ar}/39\text{Ar}$ dating of the Thorsmork ignimbrite and Icelandic sub-glacial rhyolites, *Quaternary Science Reviews*, 209, 52–62, <https://doi.org/10.1016/j.quascirev.2019.02.014>, 2019.
- 550 Jackson, S. E., Pearson, N. J., Griffin, W. L., and Belousova, E. A.: The application of laser ablation-inductively coupled plasma-mass spectrometry to in situ U-Pb zircon geochronology, *Chemical Geology*, 211, 47–69, <https://doi.org/10.1016/j.chemgeo.2004.06.017>, 2004.
- Keller, C. B., Boehnke, P., and Schoene, B.: Temporal variation in relative zircon abundance throughout Earth history, *Geochemical Perspectives Letters*, 3, 179–189, <https://doi.org/10.7185/geochemlet.1721>, 2017.
- 555 Keller, C. B., Schoene, B., and Samperton, K. M.: A stochastic sampling approach to zircon eruption age interpretation, *Geochemical Perspectives Letters*, 8, 31–35, <https://doi.org/10.7185/geochemlet.1826>, 2018.
- Keller, F., Guillong, M., Popa, R. G., and Bachmann, O.: In Situ $230\text{Th}/238\text{U}$ Geochronology of Young Volcanic Rocks on Inclusion-Bearing Ilmenite, *Geostandards and Geoanalytical Research*, 46, 465–475, <https://doi.org/10.1111/ggr.12447>, 2022.
- Kennedy, A. K., Wotzlaw, J. F., Schaltegger, U., Crowley, J. L., and Schmitz, M.: Eocene zircon reference material for microanalysis of U-Th-Pb isotopes and trace elements, *Canadian Mineralogist*, 52, 409–421, <https://doi.org/10.3749/canmin.52.3.409>, 2014.
- 560 Kirkland, C. L., Smithies, R. H., Taylor, R. J., Evans, N., and McDonald, B.: Zircon Th/U ratios in magmatic environs, *Lithos*, 212–215, 397–414, <https://doi.org/10.1016/j.lithos.2014.11.021>, 2015.
- Larsen, G.: Recent Volcanic History of the Veidivötn Fissure Swarm, Southern Iceland - an Approach to Volcanic Risk Assessment, *Journal of Volcanology and Geothermal Research*, 22, 33–58, 1984.
- 565 Lee, J. K. W., Williams, I. S., and Ellis, D. J.: Pb, U and Th diffusion in natural zircon, *letters to nature*, 390, 159–162, 1997.
- Locher, V., Popa, R. G., Guillong, M., and Bachmann, O.: Insights into caldera cycles obtained from the eruption ages and chemistry of the youngest products of Nisyros volcano, South Aegean Arc, *Journal of Volcanology and Geothermal Research*, 460, <https://doi.org/10.1016/j.jvolgeores.2025.108281>, 2025.
- Matthews, K. A., Murrell, M. T., Goldstein, S. J., Nunn, A. J., and Norman, D. E.: Uranium and Thorium Concentration and Isotopic Composition in Five Glass (BHVO-2G, BCR-2G, NKT-1G, T1-G, ATHO-G) and Two Powder (BHVO-2, BCR-2) Reference Materials, *Geostandards and Geoanalytical Research*, 35, 227–234, <https://doi.org/10.1111/j.1751-908X.2010.00080.x>, 2011.
- 570 Moles, J. D., McGarvie, D., Stevenson, J. A., Sherlock, S. C., Abbott, P. M., Jenner, F. E., and Halton, A. M.: Widespread tephra dispersal and ignimbrite emplacement from a subglacial volcano (Torfajökull, Iceland), *Geology*, 47, 577–580, <https://doi.org/10.1130/G46004.1>, 2019.



- 575 Moser, Z.: moserzoe/UThPb-ZirChron: Zenodo release UThPb- ZirChron, <https://doi.org/10.5281/zenodo.16926790>, 2025.
- Nakamura, M.: Continuous mixing of crystal mush and replenished magma in the ongoing Unzen eruption, *Geology*, 23, 807–810, <http://pubs.geoscienceworld.org/gsa/geology/article-pdf/23/9/807/3515937/i0091-7613-23-9-807.pdf>, 1995.
- Nathwani, C., Szymanowski, D., Tavazzani, L., Markovic, S., Virmond, A. L., and Chelle-Michou, C.: Controls on zircon age distributions in volcanic, porphyry and plutonic rocks, *Geochronology*, 7, 15–33, <https://doi.org/10.5194/gchron-7-15-2025>, 2025.
- 580 Noguchi, S., Toramaru, A., and Nakada, S.: Relation between microlite textures and discharge rate during the 1991–1995 eruptions at Unzen, Japan, *Journal of Volcanology and Geothermal Research*, 175, 141–155, 2008.
- Ogliore, R. C., Huss, G. R., and Nagashima, K.: Ratio estimation in SIMS analysis, *Nuclear Instruments and Methods in Physics Research, Section B: Beam Interactions with Materials and Atoms*, 269, 1910–1918, <https://doi.org/10.1016/j.nimb.2011.04.120>, 2011.
- Paton, C., Woodhead, J. D., Hellstrom, J. C., Hergt, J. M., Greig, A., and Maas, R.: Improved laser ablation U-Pb zircon geochronology through robust downhole fractionation correction, *Geochemistry, Geophysics, Geosystems*, 11, <https://doi.org/10.1029/2009GC002618>, 2010.
- 585 Piochi, M., Cantucci, B., Montegrossi, G., and Currenti, G.: Hydrothermal alteration at the san vito area of the campi flegrei geothermal system in Italy: Mineral review and geochemical modeling, *Minerals*, 11, <https://doi.org/10.3390/min11080810>, 2021.
- Pollard, T., Woodhead, J., Hellstrom, J., Engel, J., Powell, R., and Drysdale, R.: DQPB: software for calculating disequilibrium U-Pb ages, *Geochronology*, 5, 181–196, <https://doi.org/10.5194/gchron-5-181-2023>, 2023.
- 590 Popa, R. G., Guillong, M., Bachmann, O., Szymanowski, D., and Ellis, B.: U-Th zircon dating reveals a correlation between eruptive styles and repose periods at the Nisyros-Yali volcanic area, Greece, *Chemical Geology*, 555, <https://doi.org/10.1016/j.chemgeo.2020.119830>, 2020.
- Reid, M. R., Coath, C. I. D., Harrison, T. M., and McKeegan, K. D.: Prolonged residence times for the youngest rhyolites associated with Long Valley Caldera: 230Th-238U ion microprobe dating of young zircons, 50, 27–39, 1997.
- 595 Reiners, P. W., Farley, K. A., and Hickes, H. J.: He diffusion and (U-Th)/He thermochronometry of zircon: initial results from Fish Canyon Tuff and Gold Butte, *Tectonophysics*, pp. 297–308, www.elsevier.com/locate/tecto, 2002.
- Sakata, S., Hirakawa, S., Iwano, H., Danhara, T., Guillong, M., and Hirata, T.: A new approach for constraining the magnitude of initial disequilibrium in Quaternary zircons by coupled uranium and thorium decay series dating, *Quaternary Geochronology*, 38, 1–12, <https://doi.org/10.1016/j.quageo.2016.11.002>, 2017.
- 600 Schmitt, A. K.: Uranium Series Accessory Crystal Dating of Magmatic Processes, *Annual Review of Earth and Planetary Sciences*, 39, 321–349, <https://doi.org/10.1146/annurev-earth-040610-133330>, 2011.
- Schmitt, A. K., Stockli, D. F., Lindsay, J. M., Robertson, R., Lovera, O. M., and Kislitsyn, R.: Episodic growth and homogenization of plutonic roots in arc volcanoes from combined U-Th and (U-Th)/He zircon dating, *Earth and Planetary Science Letters*, 295, 91–103, <https://doi.org/10.1016/j.epsl.2010.03.028>, 2010.
- 605 Schmitt, A. K., Sliwinski, J., Caricchi, L., Bachmann, O., Riel, N., Kaus, B. J., de León, A. C., Cornet, J., Friedrichs, B., Lovera, O., Sheldrake, T., and Weber, G.: Zircon age spectra to quantify magma evolution, *Geosphere*, 19, 1006–1031, <https://doi.org/10.1130/GES02563.1>, 2023.
- Schmitz, M. D. and Bowring, S. A.: U-Pb zircon and titanite systematics of the Fish Canyon Tuff: an assessment of high-precision U-Pb geochronology and its application to young volcanic rocks, *Geochimica et Cosmochimica Acta*, 65, 2571–2587, 2001.
- 610 Schoene, B., Samperton, K. M., Eddy, M. P., Keller, G., Adatte, T., Bowring, S. A., Khadri, S. F., and Gertsch, B.: U-Pb geochronology of the Deccan Traps and relation to the end-Cretaceous mass extinction, *Science*, 347, 182–184, <https://doi.org/10.1126/science.aaa0118>, 2015.



- Sláma, J., Košler, J., Condon, D. J., Crowley, J. L., Gerdes, A., Hanchar, J. M., Horstwood, M. S., Morris, G. A., Nasdala, L., Norberg, N.,
 Schaltegger, U., Schoene, B., Tubrett, M. N., and Whitehouse, M. J.: Plešovice zircon - A new natural reference material for U-Pb and Hf
 615 isotopic microanalysis, *Chemical Geology*, 249, 1–35, <https://doi.org/10.1016/j.chemgeo.2007.11.005>, 2008.
- Smith, P. E., York, D., Chen, Y., and Evensen, N. M.: Single crystal ^{40}Ar - ^{39}Ar dating of a Late Quaternary paroxysm on Kos, Greece:
 Concordance of terrestrial and marine ages, *Geophysical Research Letters*, 23, 3047–3050, <https://doi.org/10.1029/96GL02759>, 1996.
- Stacey, J. S. and Kramers, J. D.: Approximation of terrestrial lead isotope evolution by a two-stage model, *Earth and Planetary Science
 Letters*, 26, 207–221, 1975.
- 620 Svensson, A., Andersen, K. K., Bigler, M., Clausen, H. B., Dahl-Jensen, D., Davies, S. M., Johnsen, S. J., Muscheler, R., Parrenin, F.,
 Rasmussen, S. O., Röthlisberger, R., Seierstad, I., Steffensen, J. P., and Vinther, B. M.: Climate of the Past A 60 000 year Greenland
 stratigraphic ice core chronology, *Clim. Past*, 4, 47–57, www.clim-past.net/4/47/2008/, 2008.
- Troch, J., Ellis, B. S., Schmitt, A. K., Bouvier, A. S., and Bachmann, O.: The dark side of zircon: textural, age, oxygen isotopic and
 trace element evidence of fluid saturation in the subvolcanic reservoir of the Island Park-Mount Jackson Rhyolite, Yellowstone (USA),
 625 *Contributions to Mineralogy and Petrology*, 173, <https://doi.org/10.1007/s00410-018-1481-2>, 2018.
- Turner, S., Hawkesworth, C., van Calsteren, P., Heath, E., Macdonald, R., and Black, S.: U-series isotopes and destructive plate margin
 magma genesis in the Lesser Antilles, *Earth and Planetary Science Letters*, 142, 191–207, 1996.
- Vermeesch, P.: IsoplotR: A free and open toolbox for geochronology, *Geoscience Frontiers*, 9, 1479–1493,
<https://doi.org/10.1016/j.gsf.2018.04.001>, 2018.
- 630 Vermeesch, P.: An algorithm for U–Pb geochronology by secondary ion mass spectrometry, *Geochronology*, 4, 561–576,
<https://doi.org/10.5194/gchron-4-561-2022>, 2022.
- Vermeesch, P.: KJ.jl, <https://github.com/pvermeesch/KJ.jl>, accessed: 2025-07-15, 2025.
- Watson, E. B.: Dissolution, growth and survival of zircons during crustal fusion: Kinetic principals, geological models
 and implications for isotopic inheritance, *Transactions of the Royal Society of Edinburgh, Earth Sciences*, 87, 43–56,
 635 <https://doi.org/10.1017/S0263593300006465>, 1996.
- Watson, E. B. and Harrison, T. M.: Zircon saturation revisited: temperature and composition effects in a variety of crustal magma types,
Earth and Planetary Science Letters, 64, 295–304, 1983.
- Wendt, I. and Carl, C.: The statistical distribution of the mean squared weighted deviation, *Chemical Geology (Isotope Geoscience Section)*,
 86, 275–285, 1991.
- 640 Wiedenbeck, M., Allé, P., Corfu, F., Griffin, W. L., Meier, M., Oberli, F., von Quadt, A., Roddick, J. C., and Spiegel, W.: Three Natural Zircon
 Standards for U-Th-Pb, Lu-Hf, Trace Element and REE Analyses, *Geostandards Newsletter*, 19, 1–23, <https://doi.org/10.1111/j.1751-908X.1995.tb00147.x>, 1995.